Multi-Spectral Face Recognition: Identification of People in Difficult Environments

Thirimachos Bourlai and Bojan Cukic
Lane Department of Computer Science and Electrical Engineering
West Virginia University, Morgantown, WV 26506
Email: {Thirimachos.Bourlai, Bojan.Cukic}@mail.wvu.edu

***Abstract*—In this paper we study the problems of intra-spectral and cross-spectral face recognition (FR) in homogeneous and heterogeneous environments. Specifically we investigate the advantages and limitations of matching (i) short wave infrared (SWIR) face images to visible images under controlled or uncontrolled conditions, (ii) mid-wave infrared (MWIR) to MWIR or visible images under controlled conditions, and (iii) intra-distance near infrared (NIR) to NIR images and cross-distance, cross-spectral NIR to visible images. All NIR images were captured night-time, outdoors and at mid-ranges (from 30 up to 120 meters). We utilized both commercial and academic face matchers and performed a set of experiments indicating that our cross-photometric score level fusion rule can be utilized to improve SWIR cross-spectral matching performance across all FR scenarios investigated. We also show that intra-spectral matching results, using either MWIR or NIR images, are comparable to the baseline results, i.e., when comparing visible to visible face images. Our experiments also indicate that the level of improvement in recognition performance is scenario dependent. Experiments also show that cross-spectral matching (the heterogeneous problem, where gallery and probe sets have face images acquired in different spectral bands) is a very challenging problem and it requires further investigation to address real-world law enforcement or military situations.**

I. Introduction

Biometric systems utilize physiological (face, fingerprints, iris etc.) or behavioral (keystroke dynamics etc.) traits to establish human identity. Face-based recognition (FR) systems, in particular, are gaining interest because face has several advantages over other biometric traits: it is non-intrusive, understandable, and can be captured in a covert manner at standoff distances.

A typical face recognition system includes an enrollment phase, during which images of the users' face are taken and used to create a template that is stored in a database (gallery images). During the authentication phase, newly recorded images of a user's face, called probes, are used for recognition. A decision on the person's identity is taken on the basis of the comparison between the gallery templates and the new (probe) images.

Most face recognition systems depend on the usage of face images captured in the visible range of the electromagnetic spectrum, i.e. 380-750 *nm*. However, in real-world scenarios (military and law enforcement) we have to deal with harsh environmental conditions characterized by unfavorable lighting and pronounced shadows. Such an example is a night-time environment [1], where human recognition based solely on visible spectral images may not be feasible [2], [3]. In order to deal with such difficult FR scenarios, mutli-spectral camera sensors are very useful because they can image day and night [4]. Thus, recognition of faces across the infrared spectrum has become an area of growing interest [2], [5], [6].

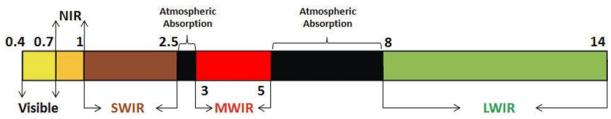

Figure 1. Electromagnetic spectrum map: face recognition research challenges across the band. The illustrated wavelengths are in μm.

The infrared (IR) spectrum is divided into different spectral bands. The boundaries between these bands can vary depending on the scientific field involved (e.g., optical radiation, astrophysics, or sensor technology [7]). The IR bands, discussed in this work, are based on the response of various detectors (see Fig. 1). Specifically, the IR spectrum is comprised of the active IR band and the thermal (passive) IR band. The active band (0.7-2.5μm) is divided into the NIR (near infrared) and the SWIR (shortwave infrared) spectrum. The SWIR has a longer wavelength range than NIR and is more tolerant to low levels of obscurants like fog and smoke. Differences in appearance between images sensed in the visible and the active IR band are due to the properties of the object being imaged.

The passive IR band is further divided into the Mid-Wave (MWIR) and the Long-Wave InfraRed (LWIR) band. MWIR ranges from 3-5μm, while LWIR ranges from 7-14μm. Both MWIR and LWIR cameras can sense temperature variations across the face at a distance, and produce thermograms in the form of 2D images. However, while both pertain to the thermal spectrum, they reveal different image characteristics of the facial skin. The difference between MWIR and LWIR is that MWIR has both reflective and emissive properties, whereas LWIR consists primarily of emitted radiation. The importance of MWIR FR has been recently discussed in [8] and some example scenarios will be discussed in this work.

A. Challenges in Difficult Environments

The performance of face recognition systems is very good when face images are acquired under favorable situations (i.e. cooperative subjects, short standoff distance, good illumination, no facial expression or occlusion etc.). However, many

law enforcement and military applications deal with *difficult face recognition scenarios*. Difficult FR scenarios involve either intra-spectral or cross-spectral matching.

In *difficult intra-spectral matching* scenarios, face images (probes) are acquired at either in the visible or the infrared (IR) band under difficult conditions, i.e. mid- or long-range standoff distances, non-cooperative subjects, night time etc. Then, these images are matched against face images in a gallery database. Gallery images are usually good quality images, for example, mug shots collected in a controlled indoors environment using a visible camera. A gallery database may also be designed to include face images acquired under challenging conditions, e.g. faces of known or unknown individuals (e.g. captured at night via a surveillance camera) that may be flagged as "suspicious" or with a potential to perform a "suspicious" activity.

In the case of *difficult cross-spectral matching* scenarios, infrared (IR) probe images are matched against a visible gallery database. In those scenarios, the probe images can be acquired under unfavorable situations, including uncooperative subjects, poor illumination, day/night-time environments, long standoff distances, and diverse atmospherics.

Figure 2 illustrates real-world intra-spectral and cross-spectral FR scenarios. In Figure 2 (a) we can see a typical matching scenario where the probe and gallery face images were acquired under controlled indoor conditions with uniform illumination. In the second raw (Figure 2 (b)), a more challenging intra-spectral matching condition is presented. It is a case of a real-world surveillance scenario, where both gallery and probe face images were acquired using a near infrared (NIR at 850 *nm*) mid-range camera with active illumination. The faces were acquired during night-time and at a 120 meter (about 394 feet) standoff distance [6].

In Figure 2 (c) and (d) we can see two typical cross-spectral matching scenarios where the gallery mug shots were acquired in the visible band under controlled conditions, while the probe images were acquired either in the short-wave [9] or the mid-wave [8] infrared band respectively. In practice, there are other similar scenarios that can be considered using different bands, e.g. the scenario where NIR probes are compared to visible images (as discussed in [10]).

What follows is a short description of the contributions of this work and an overview of the contents of this paper.

B. Goals and Contributions

In this work we investigate facial recognition on different West Virginia University datasets that were collected on variable spectra. There datasets include a mid-range, night time, visible-NIR dataset (103 subjects), a visible-MWIR dataset (50 subjects), and three visible-SWIR datasets, which encompass three different data collection scenarios, i.e. controlled, semi-controlled and uncontrolled. By utilizing all these datasets, the possibility of performing intra-spectral and cross-spectral facial matching under various scenarios is studied. As discussed above, both matching approaches are useful and can be very challenging. Cross-spectral matching is considered more challenging though due to the fact that the images that are matched come from sensors that operate in completely different bands and thus, the nature of the images and facial characteristics vary considerably.

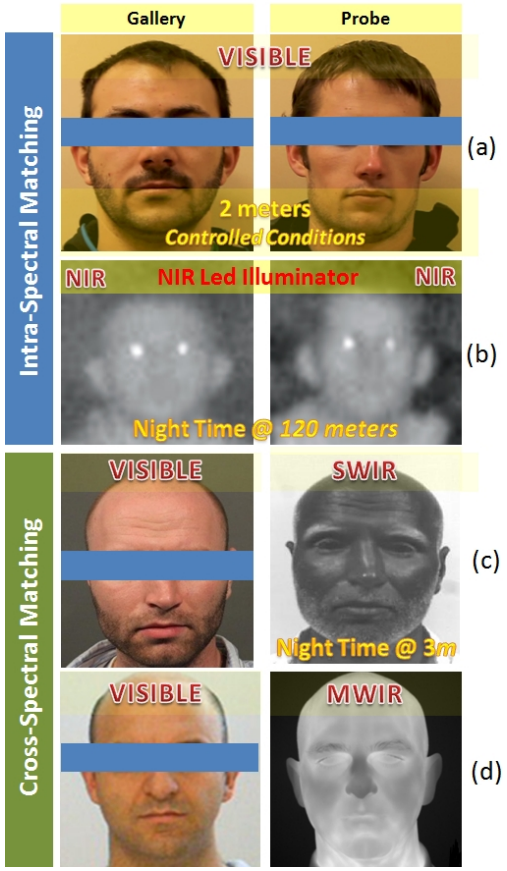

Figure 2. Real-world intra-spectral (Visible vs. Visible, or NIR vs. NIR) and cross-spectral (Visible vs. Short-Wave Infrared, or Visible vs. Mid-Wave Infrared) face recognition scenarios.

A set of experiments is performed in order to demonstrate the feasibility of intra-spectral and cross-spectral matching under controlled and challenging scenarios. First, we use the visible-SWIR datasets and we illustrate how (a) the usage of independent or combined photometric normalization techniques, and (b) cross-photometric score level fusion can be utilized to improve cross-spectral matching performance across all scenarios. This fusion approach tries to bridge the spatial representation of independent gallery (visible) and probe (SWIR) images so that we can achieve higher matching performance [9].

Second, we use the visible-MWIR dataset and we first, compare MWIR against MWIR images, and then, show that when we compare facial images captured in the MWIR spectrum with those in the visible spectrum (heterogeneous problem) the problem becomes very challenging. Finally, we use the mid-range, night time, visible-NIR dataset and we first, compare intra-distance NIR to NIR images (i.e. 30m vs. 30m images), and then cross-distance, cross-spectral images, i.e. the

baseline good quality visible images captured at controlled indoors conditions to NIR images captured at long ranges (from 30m and up to 120m).

Parts of this work were reported in [6], [8], [9]. However, in this paper, we provide an overview and a comparative study of several FR challenging scenarios that we have worked on, and we also provide new results when using face images captured at mid-ranges and at night-time environments.

C. Paper Organization

The rest of the paper is organized as follows. Section II presents the imaging modalities and the databases used in this work. Section III provides a summary of the matching approaches we employed and the experiments conducted. Finally, Section IV presents the results followed by the conclusions of this work.

II. Imaging in Difficult Environments

A. Equipment

The cameras employed for data collection in order to assemble the multi-spectral datasets described in Section I-B are listed and briefly described below.

- **Visible Cameras**: We used a Canon EOS 5D Mark II camera that has a 21.1-megapixel full-frame CMOS sensor with DIGIC 4 Image Processor and a vast ISO Range of 100-6400. It also has *Auto Lighting Optimizer* and *Peripheral Illumination Correction* that enhances its capability. In this work, Canon Mark II is used to obtain standard RGB, ultra-high resolution frontal pose face images in the visible spectrum. We also used another visible camera, i.e. the Canon PowerShot SX110, used only for the SWIR semi-controlled and uncontrolled datasets described below. It has a 9-megapixel CCD sensor with an ISO range from 80-1600.
- **SWIR Cameras**: We used the Goodrich SU640 and the XenICS Xeva-818 cameras. The SU640 is an Indium Gallium Arsenide (InGaAs) video camera featuring high sensitivity and wide dynamic range. This model has a 640×512 Focal Plane Array (FPA) with 25m pixel pitch, and a pixel operability that is higher than 99% . The spectral sensitivity of the SU640 ranges uniformly from 700 - 1700 nm wavelength. Spectral response falls rapidly at wavelengths lower than 700 nm and greater than 1700 nm. On the other hand, the Xeva-818 camera has an InGaAs 320x256 FPA with 30m pixel pitch, 98% pixel operability and three stage thermoelectric cooling. It also has a relatively uniform spectral response from 950 - 1700 nm wavelength.
- **MWIR Camera**: The camera used in this work is a high definition MWIR camera (FLIR Systems[1]). It is capable of acquiring thermal-based imprints of human skin and analyzing the thermal distributions and temporal variations, corresponding to emission of 3-5μm wavelength. The camera is capable of generating high definition thermal images and operating in diverse testing environments. It features a high resolution 1024×1024 Indium Antimonide (InSb) FPA, achieving mega-pixel image resolution in a single thermal image.
- **Near Infrared (Mid-Range) Camera**: This NIR mid-range camera leverages a focused-beam array LED technology combined with an optimized imager, optics, and a pan-tilt platform. The camera system provides high zoom magnification and long range surveillance capabilities in both day- and night-times environments. The main imaging characteristics include an 1/3" High Sensitivity Grayscale CCD with 752 x 582 (NTSC) effective pixels. The camera lens is capable for 20× continuous zoom (11 - 200 mm), with a horizontal field of view (24.1-1.4 degrees). The camera also has an IR illumination source focused LED beam array (850 nm) with an illumination power of 25w (max output).

[1]"FLIR Systems," http://www.flir.com, 2011.

B. Databases

SWIR Datasets: Three datasets were collected, i.e DB1, DB2 and DB3. **DB1** was collected in a *controlled indoor environment*, and is comprised of 50 subjects collected over two sessions. SWIR images were collected using a Xeva-818 using broadband tungsten illumination. The frontal face images were collected with and without employing a band pass filter. The wavelength of the bandpass filters starts from 950 nm and goes up to 1650 nm in steps of 100 nm. In this paper we will describe only the results when using the SWIR imagery captured at 1550 nm. The **DB2** dataset is collected in a *semi-controlled indoor environment*, composed of 50 subjects over two sessions. SWIR imagery was collected at 1550 nm with a Goodrich SU640 at a stand-off distances of 50 m and 106 m respectively, utilizing proprietary optics and laser illumination. Finally, **DB3** dataset was collected in an *uncontrolled outdoor environment* during day and night. It is composed of 16 subjects collected over multiple sessions. SWIR imagery was opportunistically collected (subjects were uncooperative, and no constraints were in place to minimize expression, pose, stand-off distance, and occlusion due to sunglasses and headgear) at 1550 nm with a Goodrich SU640 at variable stand-off distances, ranging from 60 to 400 meters.

MWIR Dataset: We used a live face capture configuration where the standoff distance was set to 6.5 feet. The database was assembled indoors spanning over a time period of 20 days. In total, 50 subjects (33 male + 17 female) participated in this experiment, and the database has 15 full frontal face MWIR images of each subject, resulting in a total of 750 MWIR images. In this dataset 750 visible images were also collected (following the above protocol using the CANON Mark II camera) to perform baseline experiments.

NIR Mid-Range Dataset: We collected face images at four standoff distances, i.e., 30, 60, 90 and 120 meters. The dataset was assembled outdoors, at night time, spanning over a time period of 20 days. Recordings of the faces of the subjects (probes) were taken with the mid-range camera, while the subjects' mug shots were taken using the CANON Mark II

camera in an indoors controlled environment. In total, 103 subjects (69 male + 34 female) participated in this experiment, and the database has video sequences of full frontal mid-range NIR and visible face images of each subject, resulting in a total of 103×5 videos (103×4 NIR outdoors and 103 visible indoors) per subject.

III. Matching in Difficult Environments

A. Face and Eye Detection Methodologies

First, the Viola & Jones face detection algorithm was applied to the visible, short-range NIR (30m) and SWIR images from the DB1, DB2, and DB3 (visible only) databases. It was used to localize the spatial extent of the face and determine its boundary. In the case of the MWIR dataset, the face area was localized by first performing binirization of the image and then blob analysis to localize the face region, while in the case of longer range NIR images face detection was performed manually. A geometric normalization scheme was applied to images acquired after face detection. The normalization scheme compensated for slight perturbations in the frontal pose, and consisted of eye detection and affine transformation.

Automated eye detection was performed when using the visible, short-range NIR (30m), SWIR [9] and MWIR [8] images. When we had to deal with challenging images, traditional face and eye detection techniques did not work, e.g. when evaluating images from DB3 acquired in the SWIR band or NIR images acquired at distance greater than 60 meters. In those cases, eyes centers were located by manual annotation. After the eye centers were found either automatically or manually, the canonical faces were automatically constructed by applying an affine transformation. Finally, all faces were canonicalized to the same dimension of 150×130 pixels.

B. Photometric Normalization Techniques

Cross-spectral SWIR face recognition is a challenging problem because the physical interaction of different electromagnetic waves (i.e., visible vs. SWIR) with materials (in our case facial skin) are different, resulting in different reflection, transmission and scattering properties. As such, texture, contrast, etc. is different when dealing with visible and SWIR face images. Photometric normalization (PN) algorithms have traditionally been employed to compensate for changes in illumination, such as ambient variation or strong shadows [11]. Similarly, in this work we employ PN for the purpose of facilitating cross-spectral matching. More specifically, we employed contrast limited adaptive histogram equalization (CLAHE) [12], single scale retinex with logarithmic (SSRlog) or with arc-tangent transformation (SSRatan), and either SSRlog or SSRatan followed by CLAHE (see Fig. 3 (middle)).

In the case of MWIR images we know that they are robust to lighting variations but their representation changes after applying different normalization techniques. Thus, for PN and in order to facilitate *intra-spectral (MWIR to MWIR) matching*, we employed the CLAHE technique. For *cross-spectral (visible vs. MWIR) matching*, among all the PN approaches evaluated, the single-scale self quotient image (SQI) and the Difference-of-Gaussian (DoG) methods were observed to be the most effective ones (see Fig. 3 (top)). Finally, mid-range NIR images after normalization are illustrated in Fig. 3 (bottom).

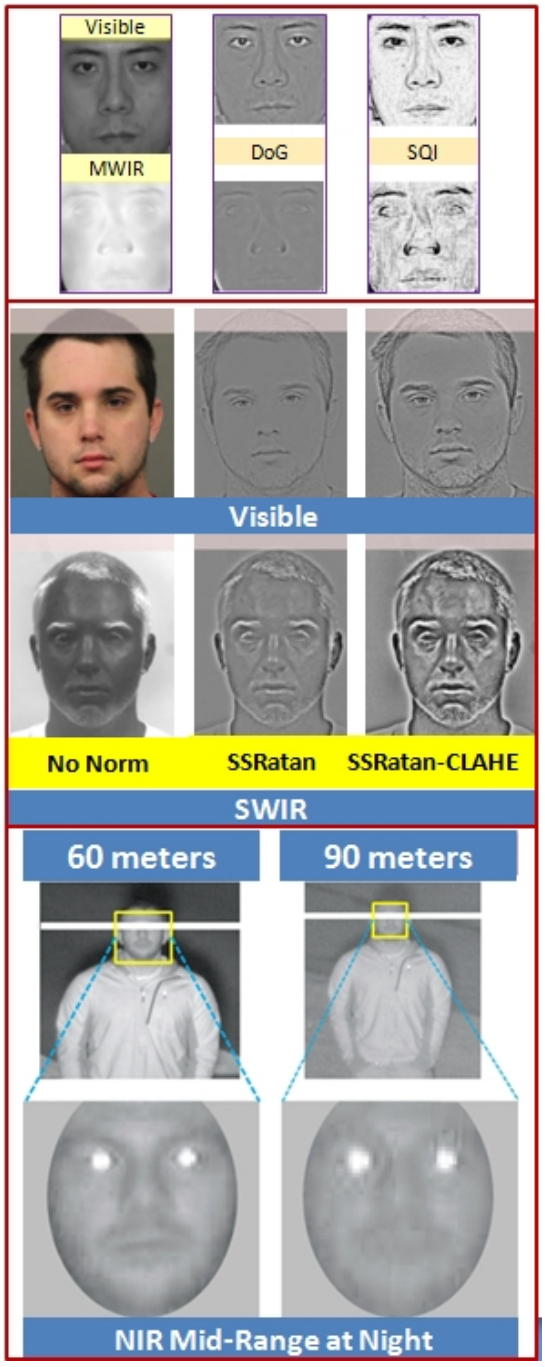

Figure 3. Multi-spectral images before and after photometric normalization: MWIR (top), SWIR (middle) and NIR (bottom).

C. Face Recognition Methods

Both commercial and academic software were employed to perform the face recognition experiments. In terms of the com-

mercial software we used the *Identity Tools G8* provided by L1 Systems[2]. This algorithm was used only for FR experiments in the visible spectrum to establish a baseline performance. In the academic software we used standard face recognition methods are provided by the CSU Face Identification Evaluation System [13], including *Principle Components Analysis* (PCA) [14]–[16], *a combined Principle Components Analysis and Linear Discriminant Analysis algorithm* (PCA+LDA) [17], and the *Bayesian Intra-personal/Extra-personal Classifier* (BIC) using either the Maximum Likelihood (ML) or the Maximum A Posteriori (MAP) hypothesis [18]. We also used two texture-based FR methods, i.e. the *Local Binary Pattern* (LBP) [19] and the *Local Ternary Pattern* (LTP) [20].

D. Matching Across Different Bands

Utilizing the datasets discussed in Section II-B we performed the following experiments. When using the *SWIR datasets* we compared the (i) visible to visible (baseline) images, (ii) visible to SWIR (before photometric normalization), and (iii) visible to SWIR when using our proposed cross-photometric fusion approach. In the case of the *MWIR dataset*, we compared the (i) visible vs. visible (baseline), (ii) MWIR vs. MWIR, and (iii) cross-spectral (visible vs. MWIR) using individual feature vectors.

Finally, when using the *NIR mid-range dataset*, we compared (i) visible vs. visible (baseline using only the L1 Systems commercial software) and (ii) intra-spectral, intra-distance NIR vs. NIR at all distances. The experiments performed were 30m vs. 30m (baseline, best quality images), 60m vs. 60m, 90m vs. 90m, and 120m vs. 120m. (iii) We also compare cross-distance, cross-spectral images, i.e. the baseline visible images to NIR images captured at 30m, 60m, 90m and 120m respectively. In both (ii) and (iii) the training set was fixed to 40%. We also used variable training sets but due to the page limitation of this paper we could not include and discuss all results.

The identification performance of the system is evaluated through the cumulative match characteristic (CMC) curve. The CMC curve measures the $1 : m$ identification system performance, and judges the ranking capability of the identification system. In Tables I, II and III below we can see a summary of all the SWIR, MWIR and NIR results respectively.

	DB1 (Controlled Indoors)	
	Visible-Visible	Visible-SWIR (w/o Norm, Proposed)
G8	1	(0.94, **1**)
LBP	0.96	(0.46, 0.56)
LTP	0.96	(0.48, 0.64)
	DB2 (Semi-Controlled Indoors) @ 50m	
	Visible-Visible	Visible-SWIR (w/o Norm, Proposed)
G8	1	(0.82, **0.90**)
LBP	1	(0.16, 0.29)
LTP	1	(0.22, 0.24)
	DB2 (Semi-Controlled Indoors) @ 106m	
	Visible-Visible	Visible-SWIR (w/o Norm, Proposed)
G8	1	(0.67, **0.80**)
LBP	1	(0.20, 0.22)
LTP	1	(0.20, 0.18)
	DB3 (Uncontrolled Outdoors) @ [60 to 400m]	
	Visible-Visible	Visible-SWIR (w/o Norm, Proposed)
G8	0.81	(0.29, **0.37**)
LBP	0.69	(0.11, 0.15)
LTP	0.69	(0.10, 0.11)

Table I
IDENTIFICATION RATES (RANK-1) FOR THE BASELINE AND CROSS-SPECTRAL (VISIBLE-SWIR@1550NM) SCENARIOS. NOTE THAT AS *Proposed* WE INDICATE OUR CROSS-PHOTOMETRIC SCORE LEVEL FUSION. W/O NORM=WITHOUT PHOTOMETRIC NORMALIZATION.

	Visible - MWIR Dataset			
ALG (PN) [SM]	v-v	mwir-mwir	v-mwir	mwir-v
G8	1	0.987	0.205	0.195
LBP (CLAHE) [CHI]	0.99	0.970	0.315	0.170
LTP (CLAHE) [CHI]	0.99	0.970	0.328	0.220
LBP (DoG)[CHI]	-		0.308	0.167
LBP (DoG)[DT]	-		0.197	0.180
LTP (DoG)[DT]	-		0.239	0.212
LTP (DoG)[CHI]	-		0.325	0.218
TPLBP (DoG)[CHI]	-		**0.539**	**0.423**
FPLBP (DoG)[CHI]	-		0.299	0.288

Table II
IDENTIFICATION RATES (RANK-1) FOR THE INTRA/CROSS-SPECTRAL SCENARIOS: (I) MWIR VS. MWIR, (II) MWIR VS. VISIBLE, AND (III) VISIBLE VS. MWIR. TPLBP=THREE-PATCH LBP [8]. SM=SIMILARITY MEASURE. DT AND CHI= DISTANCE TRANSFORM AND CHI-SQUARED DISTANCE SIMILARITY MEASURES USED FOR FEATURE MATCHING.

IV. DISCUSSION AND CONCLUSIONS

The experimental results using the SWIR datasets indicate that, although cross-spectral matching is a very challenging problem, when gallery (visible) face images are compared against SWIR face images, and all images were acquired under fully controlled conditions (DB1 dataset), the identification rate is very high (100% at rank-1) and comparable to the baseline identification rates, i.e. v-v matching experiments. When using our proposed fusion-based approach, in semi-controlled conditions (DB2 dataset) at a stand-off distance of 50m, the identification rate (90%) is reasonably comparable to the baseline rate. However, when the stand-off distance is more than doubled (106m), the identification rate at rank-1 drops another 10%, resulting in about 80% accuracy. In the most challenging (DB3 - uncontrolled) scenario, all FR matchers do not perform well, mainly because only 16 subjects were used that were not fully cooperative and were acquired under different conditions. However, G8 in combination with the proposed fusion rule, when experimenting with DB3 database, performs better than any single matcher before PN.

When using the MWIR dataset, different scenarios were tested. As expected, cross-spectral experiments resulted in markedly reduced performance. However, identification performance on MWIR imagery holds great promise under reasonable operating conditions since it appears to be comparable to that of visible (baseline) imagery. Another benefit of using

[2]www.l1id.com

	NIR Intra-Distance (m) Matching			
ALGORITHM	30-30	60-60	90-90	120-120
Bayesian ML	0.998	0.996	0.968	0.952
Bayesian MAP	0.996	0.950	0.715	0.554
LDA	0.999	0.998	0.992	0.979
PCA	0.986	0.986	0.931	0.912
	V-NIR Cross-Distance (m) Matching			
ALGORITHM	v-nir(30)	v-nir(60)	v-nir(90)	v-nir(120)
Bayesian ML	0.985	0.983	0.933	0.920
Bayesian MAP	0.988	0.985	0.939	0.922
LDA	0.981	0.912	0.912	0.870
PCA	0.983	0.977	0.941	0.910

Table III
IDENTIFICATION RATES (RANK-1) FOR THE INTRA/CROSS-DISTANCE AND CROSS-SPECTRAL SCENARIOS: (I) 30M VS. 30M, 60M VS. 60M, 90M VS. 90M, AND 120M VS. 120M, (II) VISIBLE VS. NIR[30M, 60M, 90M, AND 120M]. NIR IMAGES CAPTURED AT 30M ARE OF GREAT QUALITY AND ARE CONSIDERED HERE AS THE BASELINE NIR DATA.

MWIR is the possibility of obtaining the same recognition rates when face images are acquired in complete darkness. However, further experiments and data collections will be necessary to investigate more challenging scenarios, e.g., when subjects are wearing glasses, or images are acquired outdoors.

The night-time mid-range NIR dataset represents a very challenging and real-world FR scenario. We conducted a comprehensive data collection with a sensor capable of acquiring NIR images at standoff distances ranging from 30-120m. The data collection effort (face images of subjects were acquired with intra-personal variability) was designed to investigate the hypothesis that night time mid-range NIR imagery would yield high recognition performance at short ranges that degrades as the distance of the target to the sensor increases. Different scenarios were tested allowing us to gain some understanding of the shortcomings of such a FR scenario.

As expected, intra-spectral (NIR) intra-distance experiments resulted in a performance that reduces as a function of distance, especially at ranges greater than 90 meters, where facial features become less prominent due to various factors including atmospheric conditions. The same trend was noticed in the cross-distance cross-spectral experiments, e.g. rank-1 results, when matching visible against NIR images at 30m, were the best when compared to the usage of NIR images captured at longer ranges. It is interesting to note that even when we match visible against NIR images captured at 120m away, the rank-1 identification rate (using the Bayesian ML algorithm) reaches 92%. Generally, all rank-1 rates appear high (some matchers perform much better than others, e.g. LDA and Bayesian ML vs. PCA), but this can be explained by the fact that we were matching same session data.

In the future, further experiments will be necessary to investigate more in-depth the statistics behind the FR results when dealing with such challenging scenarios.

ACKNOWLEDGMENTS

This work is sponsored in part through a grant from the Office of Naval Research (ONR), contract N00014-09-C-0495, and support from the NSF Center for Identification Technology Research (CITeR), award number IIP-0641331. The authors are grateful to all WVU faculty and students for their great support in various parts of this work. We also like to acknowledge West Virginia High Technology Consortium (WVHTC) Foundation and specifically Dr. Brian Lemoff for assembling and providing some of the data sets utilized in this research.

REFERENCES

[1] T. Bourlai, N. Kalka, D. Cao, B. Decann, Z. Jafri, F. Nicolo, C. Whitelam, J. Zuo, D. Adjeroh, B. Cukic, J. Dawson, L. Hornak, A. Ross, and N. A. Schmid. *Ascertaining Human Identity in Night Environments*, pages 471–478. Distributed Video Sensor Networks, Springer, 2011.

[2] A. Selinger and D. A. Socolinsky. Face recognition in the dark. In *Proc. Conference on Computer Vision and Pattern Recognition Workshop*, pages 129–134, Washington, DC, USA, June 2004. IEEE.

[3] M. Ao, D. Yi, Z. Lei, and S. Z. Li. *Handbook of Remote Biometrics for Surveillance and Security*. Advances in Computer Vision and Pattern Recognition Series, Springer, 2009.

[4] T. Bourlai, N. Narang, B. Cukic, and L. Hornak. SWIR Multi-Wavelength Acquisition System for Simultaneous Capture of Face Images. In *SPIE (Vol. 8353), Infrared Technology and Applications XXXVIII*, Baltimore, U.S.A., April 2012.

[5] Y. Yoshitomi, T. Miyaura, S. Tomita, and S. Kimura. Face identification using thermal image processing. *WRHC*, pages 374–379, 1997.

[6] T. Bourlai, J. VonDollen, N. Mavridis, and C. Kolanko. Evaluating the Efficiency of a Nighttime, Middle-range Infrared Sensor for Applications in Human Detection and Recognition. In *SPIE, Infrared Imaging Systems: Design, Analysis, Modeling, and Testing XXIII*, Baltimore, U.S.A., April 2012.

[7] J. L. Miller. *Principles of Infrared Technology: A Practical Guide to the State of the Art*. Springer, 1994.

[8] T. Bourlai, A. Ross, C. Chen, and L. Hornak. A Study on using Middle-Wave Infrared Images for Face Recognition. In *SPIE, Biometric Technology for Human Identification IX*, Baltimore, U.S.A., April 2012.

[9] N. Kalka, T. Bourlai, B. Cukic, and L. Hornak. Cross-spectral Face recognition in Heterogeneous Environments: A Case Study on Matching Visible to Short-wave Infrared Imagery. In *International Joint Conference on Biometrics*, 2011.

[10] B. Klare and A. K. Jain. Heterogeneous face recognition: Matching nir to visible light images. In *Proc. Conference on Computer Vision and Pattern Recognition*, pages 1513–1516, Istanbul, Turkey, 2010.

[11] J. Short, J. Kittler, and K. Messer. A comparison of photometric normalisation algorithms for face verification. In *Face and Gesture Recognition*, page 254 259, May 2004.

[12] A. Reza. Realization of contrast limited adaptive histogram equalization (clahe) for real-time image enhancement. *VLSI Signal Processing*, 38:35–44, 2004.

[13] D. S. Bolme, J. R. Beveridge, M. L. Teixeira, and B. A. Draper. The CSU face identification evaluation system: Its purpose, features and structure. In *Proc. International Conference on Vision Systems*, pages 304 – 311, Graz, Austria, April 2003.

[14] L. Sirovich and M. Kirby. Application of the Karhunen-Loeve procedure for the characterization of human faces. *Transactions on Pattern Analysis and Machine Intelligence*, 12(1):103–108, 1990.

[15] M. Turk and A. Pentland. Eigenfaces for recognition. *Journal of Cognitive Neuroscience*, 3(1):71–86, 1991.

[16] A. P. Devijver and J. Kittler. *Pattern recognition: A statistical approach*. Prentice-Hall, Englewood Cliffs, N. J., 1982.

[17] P.N. Belhumeur, J. Hespanha, and D. J. Kriegman. Eigenfaces vs. fisherfaces: Recognition using class specific linear projection. *Transactions on Pattern Analysis and Machine Intelligence*, 19:45–58, 1996.

[18] M. Teixeira. The bayesian intrapersonal/extrapersonal classifier. Master's thesis, Colorado State University, Fort Collins, Colorado 80523 U.S.A., 2003.

[19] M. Pietikinen. Image analysis with local binary patterns. In *Scandinavian Conference on Image Analysis*, pages 115 – 118, June 2005.

[20] X. Tan and B. Triggs. Enhanced local texture feature sets for face recognition under difficult lighting conditions. *Trans. Img. Proc.*, 19:1635–1650, June 2010.